

## Deuteron Diffractive Dissociation

A.C.B. ANTUNES and F. CARUSO

*Centro Brasileiro de Pesquisas Físicas, Rua Dr. Xavier Sigaud 150, Rio de Janeiro, 22290, RJ, Instituto de Física, Universidade Federal do Rio de Janeiro, Caixa Postal 68528, Rio de Janeiro, 21944, RJ and Instituto de Física, Universidade do Estado do Rio de Janeiro, Rua São Francisco Xavier 524, Rio de Janeiro, 20550, RJ, Brasil*

Recebido em 24 de agosto de 1984

**Abstract** Deuteron diffractive dissociation is studied in the framework of the Three Components Deck Model. The applicability of this model to light nuclei diffractive dissociation is assumed. The existence of a slope-mass-cos  $\theta$  correlation is pointed out. The relevant distributions are obtained.

### 1. INTRODUCTION

In this paper we present an analysis of the diffractive dissociation of the deuteron,  $p+d \rightarrow p+n+p$ . The description of this reaction is done through the Three Components Deck Model (TCDM)<sup>1</sup>. This model has been introduced to describe the hadronic diffractive dissociation reactions (DDR) as  $a+b \rightarrow (1+2)+3$ . The TCDM has been able to describe the characteristic features of the DDR and, among these, the model describes very well the slope-mass-correlations<sup>3,4</sup>.

The TCDM has been extensively applied to several types of DDR, with different spin and parity structures in the dissociative vertex ( $a \rightarrow 1+2$ ). In this work we intend to suggest that the TCDM can be applied also to light nuclei dissociations (in our case the deuteron). The idea subjacent to our expectation is the principle of nuclear democracy<sup>5</sup> among nucleons and nuclei, proposed for the strong interactions.

In the three components of the TCDM there appear the dissociative vertex' of the deuteron<sup>6</sup>  $\bar{d} \rightarrow p+n$ . Each component has one particle of this vertex off mass shell. In order to find the form of the coupling in this vertex we make some approximations. We assume that all the particles are on shell and that the deuteron is an structureless particle. We neglect the small contribution of the D wave to the wave function of the deuteron.

The reason for these assumptions is that the introduction of form factors in the TCDM to take into account the off mass shell ef-

fects, could destroy the sensitive interferences among the components of the model<sup>1</sup>. These interferences are the mechanisms that describe the slope mass correlations.

Then the off mass shell and form factor effects are introduced by adjusting the parameters of the TCDM, as the elastic diffractive slopes (B) and the asymptotic total cross sections  $\sigma_{\text{tot}}(\infty)$ , which appear in each component. These parameters are fitted with values near the on shell experimental ones.

Another motivation to apply the TCDM to the deuteron diffractive break up is the inexistence of proton-neutron resonances, in the energy range considered. In general the TCDM, even in its simplest formulation, is valid only for low energies ( $\sqrt{s_1}$ ) of the dissociated subsystem (1+2), below the threshold of resonance formation. For higher energies the model must be reggeized and dualized<sup>1,4</sup>, in order to describe the high energy behaviour of dissociation.

As for deuteron diffractive dissociation there are no resonances in the dissociated subsystem (proton-neutron) the model is expected to be valid in a larger range of energy than in those cases in which resonances do exist. The TCDM is constructed with the Born terms of proton and neutron exchange and deuteron direct pole, which are sufficient to describe the low energy behaviour of dissociation. Reggeization and dualization that describe the high energy behaviour correspond to introducing the necessary corrections in the Born approximations.

In the next section the helicity amplitudes, which describe the deuteron diffractive dissociation using the TCDM, are presented. In section 3 the numerical results are discussed and some conclusions are presented. In the Appendix we define useful variables and expressions needed to describe the TCDM.

## 2. THE APPLICATION OF THREE COMPONENT DECK MODEL TO DEUTERON BREAK UP

The helicity amplitude of deuteron break up, given by the TCDM, is the coherent sum of the Born terms showed in fig. A2. Following the prescriptions to write the components of the model given in reference<sup>3b</sup>, and using the kinematical results shown in the Appendix, we have for the s-component:

$$A_{\lambda_1 \lambda_2 \lambda_\alpha}^{(s)} = S \bar{u}(p_1, \lambda_1) \Gamma_{(dNN)}^H v(-p_2, -\lambda_2) \left\{ -g_{\mu\nu} + \frac{p_\mu p_\nu}{p^2} \right\} \\ \times R_\beta \Gamma_{(Pd)}^{\nu\beta\rho} \varepsilon_\rho(p_\alpha, \lambda_\alpha) \quad (1)$$

where

$$S = i g^s(t_2) / (m_d^2 - s_1) \quad (2)$$

with

$$g^s(t_2) = \sigma_{\text{tot}}^{(Nd)} e^{B_{Nd} t_2 / 2} \quad (3)$$

and

$$\Gamma_{(dNN)}^H = \gamma^H + (p_1 - p_2)^H / 4m \quad (4)$$

which is the dissociative vertex of deuteron into nucleons<sup>6</sup>, neglecting the D wave contribution to the deuteron wave function.  $m_d$  and  $m$  are respectively the deuteron and nucleon masses, and

$$\Gamma_{(Pd)}^{\nu\beta\rho} = 2(g^{\nu\beta} K^\rho + K^\nu g^{\beta\rho}) - g^{\nu\rho} K^\beta \quad (5)$$

is the helicity conserving Pomeron-deuteron coupling<sup>4,7</sup>. The u-component is

$$A_{\lambda_1 \lambda_2 \lambda_\alpha}^{(u)} = U \bar{u}(p_1, \lambda_1) \not{K} (K+m) \Gamma_{(dNN)}^\alpha v(-p_2, -\lambda_2) \varepsilon_\alpha(p_\alpha, \lambda_\alpha) \quad (6)$$

where

$$U = i g^u(t_2) / (m^2 - u_1) \quad (7)$$

$$g^u(t_2) = \sigma_{\text{tot}}^{NN} e^{B_{NN} t_2 / 2} \quad (8)$$

and

$$\Gamma_{(dNN)}^\alpha = \gamma^\alpha + (p_2 - k)^\alpha / 4m \quad (9)$$

And the t-component reads

$$A_{\lambda_1 \lambda_2 \lambda_\alpha}^{(t)} = T \bar{u}(p_2, \lambda_2) \not{\not{A}} (\not{A}+m) \Gamma_{(dNN)}^\alpha v(-p_1, -\lambda_1) \varepsilon_\alpha(p_\alpha, \lambda_\alpha) \quad (10)$$

where

$$T = i g^t(t_2) / (m^2 - t_1) \quad (11)$$

$$g^t(t_2) = \sigma_{\text{tot}}^{NN} e^{B_{NN}t_2/2} \quad (12)$$

and

$$\Gamma_{(dNN)}^\alpha = \gamma^\alpha + (p_1 - q)^\alpha / 4m \quad (13)$$

In the high energy approximations, where  $s, s_2, s_3 \gg s_1, |t_1|, |u_1|, |t_2|, m_d^2, m^2$ , these components become

$$\begin{aligned} A_{\lambda_1 \lambda_2 \lambda_\alpha}^{(s)} &\approx \frac{s}{2} S \bar{u}(p_1, \lambda_1) \left\{ \frac{1}{8m\sqrt{s_1}} \left[ \left[ -(2s_1 + u_1 - t_1) \right. \right. \right. \\ &+ 4s_1 s_2 / s \left. \right] \varepsilon^0(p_\alpha \lambda_\alpha) + (u_1 - t_1) (\text{sen} \alpha \varepsilon^1(p_\alpha \lambda_\alpha) + \cos \alpha \varepsilon^3(p_\alpha \lambda_\alpha)) \left. \right] \\ &- \vec{p}_1 \cdot \vec{\varepsilon}(p_\alpha \lambda_\alpha) / 2m + (\text{sen} \alpha \varepsilon^0(p_\alpha \lambda_\alpha) - \varepsilon^1(p_\alpha \lambda_\alpha)) \gamma^1 - \varepsilon^2(p_\alpha \lambda_\alpha) \gamma^2 \\ &+ \left[ (\cos \alpha + |\vec{p}_\alpha| / \sqrt{s_1}) \varepsilon^0(p_\alpha \lambda_\alpha) - (|\vec{p}_\alpha| \text{sen} \alpha / \sqrt{s_1}) \varepsilon^1(p_\alpha \lambda_\alpha) \right. \\ &\left. - (1 + |\vec{p}_\alpha| \cos \alpha / \sqrt{s_1}) \varepsilon^3(p_\alpha \lambda_\alpha) \right] \gamma^3 \} v(-p_2, -\lambda_2) \end{aligned} \quad (14)$$

$$\begin{aligned} A_{\lambda_1 \lambda_2 \lambda_\alpha}^{(u)} &\approx U \bar{u}(p_1, \lambda_1) \left[ s_3 + i s \frac{|\vec{p}_\alpha|}{2\sqrt{s_1}} \text{sen} \alpha (\text{sen} \alpha \sigma^{03} \right. \\ &\left. + \sigma^{31} - \cos \alpha \sigma^{01}) \right] (\gamma^\beta + p_2^\beta / 2m) v(-p_2, -\lambda_2) \varepsilon_\beta(p_\alpha \lambda_\alpha) \end{aligned} \quad (15)$$

and

$$\begin{aligned} A_{\lambda_1 \lambda_2 \lambda_\alpha}^{(t)} &\approx T \bar{u}(p_2, \lambda_2) \left[ s_2 + i s \frac{|\vec{p}_\alpha|}{2\sqrt{s_1}} \text{sen} \alpha (\text{sen} \alpha \sigma^{03} \right. \\ &\left. + \sigma^{31} - \cos \alpha \sigma^{01}) \right] (\gamma^\beta + p_1^\beta / 2m) v(-p_1, -\lambda_1) \varepsilon_\beta(p_\alpha \lambda_\alpha) \end{aligned} \quad (16)$$

Calculating the spin 1/2 and spin 1 wave functions in the Gottfried-Jackson system, defined in the Appendix, these amplitudes become.

For  $\lambda_\alpha = 0$

$$\begin{aligned}
 A_{\lambda_1 \lambda_2, 0}^{(s)} &\approx \frac{sS}{2m_\alpha} \{-2\lambda_2 |\vec{p}_\alpha| \sin \alpha [(E_1+m) + 4\lambda_1 \lambda_2 (E_1-m)] \\
 &\times [2\lambda_1 \sin \theta \cos(2\lambda_1 \phi) \delta_{\lambda_1 \lambda_2} + (\cos^2(\theta/2) - \sin^2(\theta/2) e^{-i4\lambda_1 \phi}) \delta_{\lambda_1, -\lambda_2}] \\
 &- 2\lambda_2 [|\vec{p}_\alpha| (\cos \alpha + |\vec{p}_\alpha|/\sqrt{s_1}) - E_\alpha (1 + |\vec{p}_\alpha| \cos \alpha/\sqrt{s_1})] \cdot [(E_1+m) + 4\lambda_1 \lambda_2 (E_1-m)] \\
 &\times [2\lambda_2 \cos \theta \delta_{\lambda_1 \lambda_2} - \sin \theta e^{-2i\lambda_1 \phi} \delta_{\lambda_1, -\lambda_2}] \} \quad (17)
 \end{aligned}$$

$$\begin{aligned}
 A_{\lambda_1 \lambda_2, 0}^{(u)} &\approx \frac{U}{m_\alpha} \{-2|\vec{p}_1| |\vec{p}_\alpha| (s_3 - sE_\alpha \sin^2 \alpha / 2\sqrt{s_1}) \delta_{\lambda_1 \lambda_2} \\
 &+ 2\lambda_2 (s_3 E_\alpha - s |\vec{p}_\alpha|^2 \sin^2 \alpha / 2\sqrt{s_1}) [(E_1+m) + 4\lambda_1 \lambda_2 (E_1-m)] [2\lambda_1 \cos \theta \delta_{\lambda_1 \lambda_2} \\
 &- \sin \theta e^{-i2\lambda_1 \phi} \delta_{\lambda_1, -\lambda_2}] - 2\lambda_2 [s |\vec{p}_\alpha| \sin \alpha (E_\alpha - |\vec{p}_\alpha| \cos \alpha) / 2\sqrt{s_1}] \\
 &\times [(E_1+m) + 4\lambda_1 \lambda_2 (E_1-m)] [2\lambda_1 \sin \theta \cos(2\lambda_1 \phi) \delta_{\lambda_1 \lambda_2} + (\cos^2(\theta/2) \\
 &- \sin^2(\theta/2) e^{-i4\lambda_1 \phi}) \delta_{\lambda_1, -\lambda_2}] + i(s |\vec{p}_\alpha| \sin \alpha / 2\sqrt{s_1}) \{-4\lambda_2 (\lambda_1 + \lambda_2) |\vec{p}_1| \\
 &\times (|\vec{p}_\alpha| - E_\alpha \cos \alpha) [\sin \theta \sin(2\lambda_1 \phi) \delta_{\lambda_1 \lambda_2} - 2i\lambda_1 (\cos^2(\theta/2) \\
 &+ \sin^2(\theta/2) e^{-i4\lambda_1 \phi}) \delta_{\lambda_1, -\lambda_2}] + (E_\alpha |\vec{p}_\alpha| + |\vec{p}_1| E_\alpha \cos \alpha) [-i2\lambda_2 \\
 &\times \sin \alpha [(E_1+m) - 4\lambda_1 \lambda_2 (E_1-m)] [2\lambda_1 \cos \theta \delta_{\lambda_1 \lambda_2} - \sin \theta e^{-i2\lambda_1 \phi} \delta_{\lambda_1, -\lambda_2}] / 2m \\
 &- 4\lambda_2 (\lambda_2 - \lambda_1) |\vec{p}_1| [\sin \theta \sin(2\lambda_1 \phi) \delta_{\lambda_1 \lambda_2} - 2i\lambda_1 (\cos^2(\theta/2) \\
 &+ \sin^2(\theta/2) e^{-i4\lambda_1 \phi}) \delta_{\lambda_1, -\lambda_2}] + 2i\lambda_2 \cos \alpha [(E_1+m) - 4\lambda_1 \lambda_2 (E_1-m)] \\
 &\times [2\lambda_1 \sin \theta \cos(2\lambda_1 \phi) \delta_{\lambda_1 \lambda_2} + (\cos^2(\theta/2) - \sin^2(\theta/2) e^{-i4\lambda_1 \phi}) \delta_{\lambda_1, -\lambda_2}] \} \} \quad (18)
 \end{aligned}$$

$$\begin{aligned}
A_{\lambda_1 \lambda_2 0}^{(t)} \approx & \frac{T}{m_\alpha} \{ -2 |\vec{p}_1| |\vec{p}_\alpha| (s_2 - s E_\alpha \sin^2 \alpha / 2\sqrt{s_1}) \delta_{\lambda_1 \lambda_2} \\
& + 2\lambda_1 (s_2 E_\alpha - s |\vec{p}_\alpha|^2 \sin^2 \alpha / 2\sqrt{s_1}) [(E_1 + m) + 4\lambda_1 \lambda_2 (E_1 - m)] [-2\lambda_2 \cos \theta \delta_{\lambda_1 \lambda_2} \\
& + \sin \theta e^{-i2\lambda_2 \phi} \delta_{\lambda_2, -\lambda_1}] - 2\lambda_1 [s |\vec{p}_\alpha| \sin \alpha (E_\alpha - |\vec{p}_\alpha| \cos \alpha) / 2\sqrt{s_1}] \\
& \times [(E_1 + m) + 4\lambda_1 \lambda_2 (E_1 - m)] [-2\lambda_2 \sin \theta \cos(2\lambda_2 \phi) \delta_{\lambda_1 \lambda_2}^2 + (\sin^2(\theta/2) \\
& - \cos^2(\theta/2)) e^{-i4\lambda_2 \phi} \delta_{\lambda_2, -\lambda_1}] + i (s |\vec{p}_\alpha| \sin \alpha / 2\sqrt{s_1}) \{-4\lambda_1 (\lambda_1 + \lambda_2) |\vec{p}_1| \\
& \times (|\vec{p}_\alpha|^{-E_\alpha \cos \alpha}) [-\sin \theta \sin(2\lambda_2 \phi) \delta_{\lambda_1 \lambda_2} - i2\lambda_2 (\sin^2(\theta/2) \\
& + \cos^2(\theta/2)) e^{-i4\lambda_2 \phi} \delta_{\lambda_2, -\lambda_1}] \\
& + (E_1 |\vec{p}_\alpha| - |\vec{p}_1| E_\alpha \cos \theta) [-i2\lambda_1 \sin \alpha [(E_1 + m) - 4\lambda_1 \lambda_2 (E_1 - m)] [-2\lambda_2 \cos \theta \delta_{\lambda_1 \lambda_2}^2 \\
& + \sin 8 e^{-i2\lambda_2 \phi} \delta_{\lambda_2, -\lambda_1}] - 4\lambda_1 (\lambda_1 - \lambda_2) |\vec{p}_1| [-\sin 8 \sin(2\lambda_2 \phi) \delta_{\lambda_1 \lambda_2}^2 \\
& - 2i\lambda_2 (\sin^2(\theta/2) + \cos^2(\theta/2)) e^{-i4\lambda_2 \phi} \delta_{\lambda_2, -\lambda_1}] \\
& + 2i\lambda_1 \cos \alpha [(E_1 + m) - 4\lambda_1 \lambda_2 (E_1 - m)] [-2\lambda_2 \sin \theta \cos(2\lambda_2 \phi) \delta_{\lambda_1 \lambda_2} \\
& + (\sin^2(\theta/2) - \cos^2(\theta/2)) e^{-i4\lambda_2 \phi} \delta_{\lambda_2, -\lambda_1}] \} \} \quad (19)
\end{aligned}$$

and for  $\lambda_\alpha = \pm 1$

$$\begin{aligned}
A_{\lambda_1 \lambda_2, \lambda_\alpha = \pm 1}^{(s)} \approx & (-\lambda_2 \lambda_\alpha s S / \sqrt{2}) [(E_1 + m) + 4\lambda_1 \lambda_2 (E_1 - m)] \\
& \times \{ 2\lambda_1 \sin \theta \cos(2\lambda_1 \phi) \delta_{\lambda_1 \lambda_2} + (\cos^2(\theta/2) - \sin^2(\theta/2)) e^{-i4\lambda_1 \phi} \delta_{\lambda_1, -\lambda_2} \\
& + i\lambda_\alpha \sin 8 \sin(2\lambda_1 \phi) \delta_{\lambda_1 \lambda_2} + 2\lambda_\alpha \lambda_1 (\cos^2(\theta/2) \\
& + \sin^2(\theta/2)) e^{-i4\lambda_1 \phi} \delta_{\lambda_1, -\lambda_2} + (|\vec{p}_\alpha| s \sin \alpha / \sqrt{s_1}) (2\lambda_1 \cdot \cos \theta \delta_{\lambda_1 \lambda_2} \\
& - \sin \theta e^{-i2\lambda_1 \phi} \delta_{\lambda_1, -\lambda_2}) \} \quad (20)
\end{aligned}$$

$$\begin{aligned}
A_{\lambda_1 \lambda_2, \lambda_\alpha}^{(u)} = \pm 1 &\approx (\lambda_\alpha u / \sqrt{2}) \{-2\lambda_2 s_3 [(E_1 + m) + 4\lambda_1 \lambda_2 (E_1 - m)] \\
&\times \{ [2\lambda_1 \sin \theta \cos(2\lambda_1 \phi) \delta_{\lambda_1 \lambda_2} + (\cos^2(\theta/2) - \sin^2(\theta/2) e^{-i4\lambda_1 \phi}) \delta_{\lambda_1, -\lambda_2}] \\
&+ i\lambda_\alpha [\sin \theta \sin(2\lambda_1 \phi) \delta_{\lambda_1 \lambda_2} - 2i\lambda_1 (\cos^2(\theta/2) + \sin^2(\theta/2) e^{-i4\lambda_1 \phi}) \delta_{\lambda_1, -\lambda_2}] \} \\
&+ (is |\vec{p}_\alpha| \sin \alpha / 2\sqrt{s_1}) \{ i \cos \alpha [-2 |\vec{p}_1| \delta_{\lambda_1 \lambda_2} + 4\lambda_\alpha \lambda_2 (\lambda_1 + \lambda_2) |\vec{p}_1| \\
&\times (2\lambda_1 \cos \theta \delta_{\lambda_1 \lambda_2} - \sin \theta e^{-i2\lambda_1 \phi} \delta_{\lambda_1, -\lambda_2})] + 4\lambda_2 (\lambda_1 + \lambda_2) |\vec{p}_1| \sin \alpha \\
&\times [-\sin \theta \sin(2\lambda_1 \phi) \delta_{\lambda_1 \lambda_2} + 2i\lambda_1 (\cos^2(\theta/2) + \sin^2(\theta/2) e^{-i4\lambda_1 \phi}) \delta_{\lambda_1, -\lambda_2} \\
&+ i\lambda_\alpha (2\lambda_1 \sin \theta \cos(2\lambda_1 \phi) \delta_{\lambda_1 \lambda_2} + (\cos^2(\theta/2) - \sin^2(\theta/2) e^{-i4\lambda_1 \phi}) \delta_{\lambda_1, -\lambda_2}) \} \\
&+ i[-4\lambda_\alpha \lambda_1 E_1 \delta_{\lambda_1 \lambda_2} + 2\lambda_2 [(E_1 + m) + 4\lambda_1 \lambda_2 (E_1 - m)] (2\lambda_1 \cos \theta \delta_{\lambda_1 \lambda_2} \\
&- \sin \theta e^{-i2\lambda_1 \phi} \delta_{\lambda_1, -\lambda_2})] - (|\vec{p}_1| / 2m) \sin \theta e^{i\lambda_\alpha \phi} \\
&\times \{ 2i\lambda_2 [(E_1 + m) - 4\lambda_1 \lambda_2 (E_1 - m)] \{-\sin \alpha (2\lambda_1 \cos \theta \delta_{\lambda_1 \lambda_2} \\
&- \sin \theta e^{-i2\lambda_1 \phi} \delta_{\lambda_1, -\lambda_2}) + \cos \alpha [2\lambda_1 \sin \theta \cos(2\lambda_1 \phi) \delta_{\lambda_1 \lambda_2} \\
&+ \cos^2(\theta/2) - \sin^2(\theta/2) e^{-i4\lambda_1 \phi}) \delta_{\lambda_1, -\lambda_2}] \} - 4\lambda_2 (\lambda_1 - \lambda_2) |\vec{p}_1| \\
&\times [\sin \theta \sin(2\lambda_1 \phi) \delta_{\lambda_1 \lambda_2} - 2i\lambda_1 (\cos^2(\theta/2) + \sin^2(\theta/2) e^{-i4\lambda_1 \phi}) \delta_{\lambda_1, -\lambda_2}] \} \} \\
&\text{and} \\
A_{\lambda_1, \lambda_2, \lambda_\alpha}^{(t)} = \pm 1 &\approx (\lambda_\alpha T / \sqrt{2}) \{-2\lambda_1 s_2 [(E_1 + m) + 4\lambda_1 \lambda_2 (E_1 - m)] \\
&\times \{ [-2\lambda_2 \sin \theta \cos(2\lambda_2 \phi) \delta_{\lambda_1 \lambda_2} + (\sin^2(\theta/2) - \cos^2(\theta/2) e^{-i4\lambda_2 \phi}) \delta_{\lambda_1, -\lambda_2}] \\
&- i\lambda_\alpha [\sin \theta \sin(2\lambda_2 \phi) \delta_{\lambda_1 \lambda_2} + 2i\lambda_2 (\sin^2(\theta/2) + \cos^2(\theta/2) e^{-i4\lambda_2 \phi}) \delta_{\lambda_2, -\lambda_1}] \} \\
&+ (is |\vec{p}_\alpha| \sin \alpha / 2\sqrt{s_1}) \{ i \cos \alpha [-2 |\vec{p}_1| \delta_{\lambda_1 \lambda_2} + 4\lambda_\alpha \lambda_1 (\lambda_1 + \lambda_2) |\vec{p}_1|
\end{aligned}$$

$$\begin{aligned}
& \times (-2\lambda_2 \cos \theta \delta_{\lambda_1 \lambda_2} + \sin \theta e^{-i2\lambda_2 \phi} \delta_{\lambda_2, -\lambda_1}) + 4\lambda_1(\lambda_1 + \lambda_2) |\vec{p}_1| \sin \alpha \\
& \times [\sin \theta \sin(2\lambda_2 \phi) \delta_{\lambda_1 \lambda_2} + 2i\lambda_2 (\sin^2(\theta/2) + \cos^2(\theta/2) e^{-i4\lambda_2 \phi}) \delta_{\lambda_2, -\lambda_1} \\
& + i\lambda_\alpha (-2\lambda_2 \sin \theta \cos(2\lambda_2 \phi) \delta_{\lambda_1 \lambda_2} + (\sin^2(\theta/2) - \cos^2(\theta/2) e^{-i4\lambda_2 \phi}) \delta_{\lambda_2, -\lambda_1}] \\
& + i[-4\lambda_\alpha \lambda_2 E_1 \delta_{\lambda_1 \lambda_2} + 2\lambda_1 |(E_1 + m) + 4\lambda_1 \lambda_2 (E_1 - m)| (-2\lambda_2 \cos \theta \delta_{\lambda_1 \lambda_2} \\
& + \sin \theta e^{-i2\lambda_2 \phi} \delta_{\lambda_2, -\lambda_1})] + (|\vec{p}_1|/2m) \sin \theta e^{i\lambda_\alpha \phi} \\
& \times \{2i\lambda_1 [(E_1 + m) - 4\lambda_1 \lambda_2 (E_1 - m)] \{ \sin \alpha (2\lambda_2 \cos \theta \delta_{\lambda_1 \lambda_2} \\
& - \sin \theta e^{-i2\lambda_2 \phi} \delta_{\lambda_2, -\lambda_1}) + \cos \alpha [-2\lambda_2 \sin \theta \cos(2\lambda_2 \phi) \delta_{\lambda_1 \lambda_2} \\
& + (\sin^2(\theta/2) - \cos^2(\theta/2) e^{-i4\lambda_2 \phi}) \delta_{\lambda_2, -\lambda_1}] \} \\
& + 4\lambda_1(\lambda_1 - \lambda_2) |\vec{p}_1| [\sin \theta \sin(2\lambda_2 \phi) \delta_{\lambda_1 \lambda_2} + 2i\lambda_2 (\sin^2(\theta/2) \\
& + \cos^2(\theta/2) e^{-i4\lambda_2 \phi}) \delta_{\lambda_2, -\lambda_1}] \} \} \} \quad (22)
\end{aligned}$$

The subreaction  $\mathbb{P}d \rightarrow pn$ , as appears in fig. A1, is submitted to some constraints due to isospin conservation. As the Pomeron has the vacuum quantum numbers, and the deuteron in an isosinglet, the initial state  $|\mathbb{P}, d\rangle$  is a  $|I=0, I_3=0\rangle$  isospin state. Then, by isospin conservation, valid in the strong interactions, the final state  $|p, n\rangle$  must also be an isosinglet  $|I=0, I_3=0\rangle$ .

As the complete space, spin and isospin wave function, in this case, must be antisymmetric under exchange of the particles, and the isosinglet is antisymmetric, the space and spin part must be symmetric. Thus, the helicity amplitudes (17 to 22) must be symmetrized before computing the cross-sections. To do this we define

$$\tilde{A}_{\lambda_1 \lambda_2 \lambda_\alpha}(\theta, \phi) = \frac{1}{2} \{ A_{\lambda_1 \lambda_2 \lambda_\alpha}(\theta, \phi) + A_{\lambda_2 \lambda_1 \lambda_\alpha}(\pi - \theta, \phi - \pi) \} \quad (23)$$

and so the symmetric helicity amplitudes are obtained in a straightforward way.



### 3. RESULTS AND DISCUSSION

The differential cross sections were calculated in the Gottfried-Jackson system, whose coordinates are shown in fig. A3, using eq. (A10).

Figs. 1 and 2 show that the main part of the events must occur for values of the effective mass  $M_{pn}$  very near the threshold, and for small angles symmetrically forward and backward in the GJS. The first distribution shows a *peak* that is a consequence of the deuteron pole, very near the threshold, in the unphysical region.

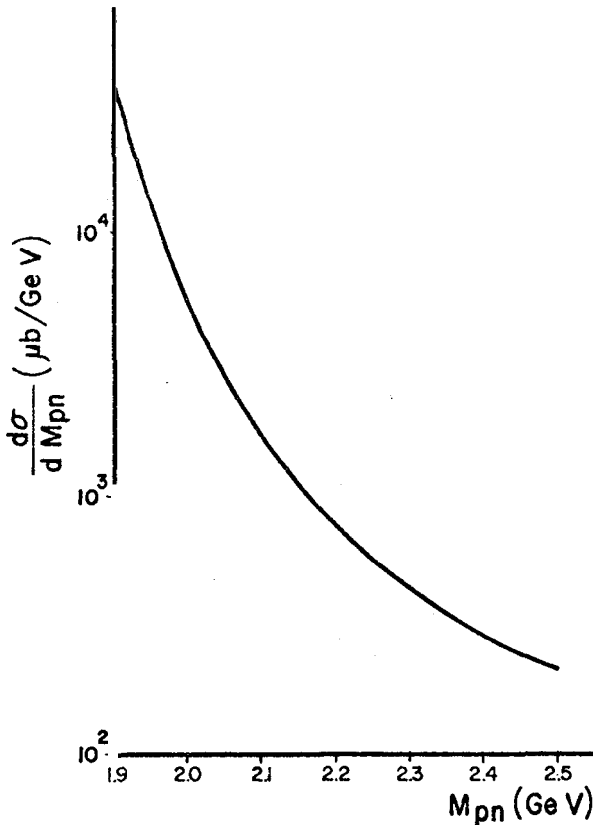


Fig.1 - Effective mass ( $M_{pn}$ ), distribution, integrated in  $\phi(0, 2\pi)$ ,  $\cos \theta (-1.0, 1.0)$  and  $t_2 (0, -1.0)$ .

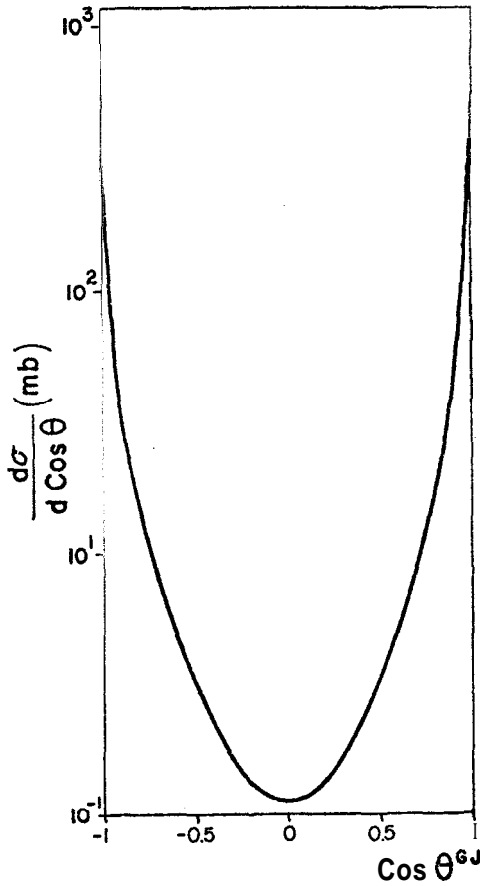


Fig.2 -  $d\sigma/d \cos \theta$  distribution, integrated in  $\phi(0,2\pi)$ ,  $t_2(0,-1.0)$  and  $M_{pn}(1.92, 2.22 \text{ (GeV)})$ .

Figs. 3 to 6 show the strong slope ( $\beta$ )-mass ( $M_{pn}$ )- $\cos \theta$  correlation that occur in this reaction. The distributions presented correspond to two effective mass interval  $1.92 < M_{pn} \leq 2.22 \text{ (GeV)}$  and  $2.22 \leq M_{pn} \leq 2.52 \text{ (GeV)}$ , and to three intervals of  $\cos \theta$ :  $-1 \leq \cos \theta \leq -0.9$ ,  $-0.3 \leq \cos \theta \leq 0.3$  and  $0.9 \leq \cos \theta \leq 1$ .

Figs. 4 and 6 show diffractive peaks whose slope decrease as the mass range increases. On the other hand, figs. 3 and 5 show interference structures, with a dip at  $t_2 = 0$ , that become smooth as the mass increases.

The effective mass interval of figs. 3 and 4 is subdivided in figs 7 to 12. Figs. 7, 9 and 11 show separately the contributions to the structure that appear in fig. 3. These figures (7 to 12) show also the slope-mass- $\cos \theta$  correlation in a mass range nearest the threshold.

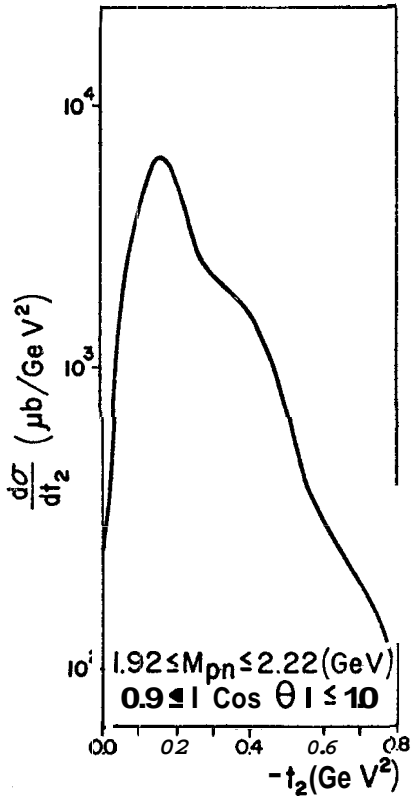


Fig.3 -  $d\sigma/dt_2$  distribution, integrated in  $\phi(0,2\pi)$ ,  $M_{pn}$  (1.92, 2.22 (GeV)) and  $|\cos \theta|$  (0.9,1.0).

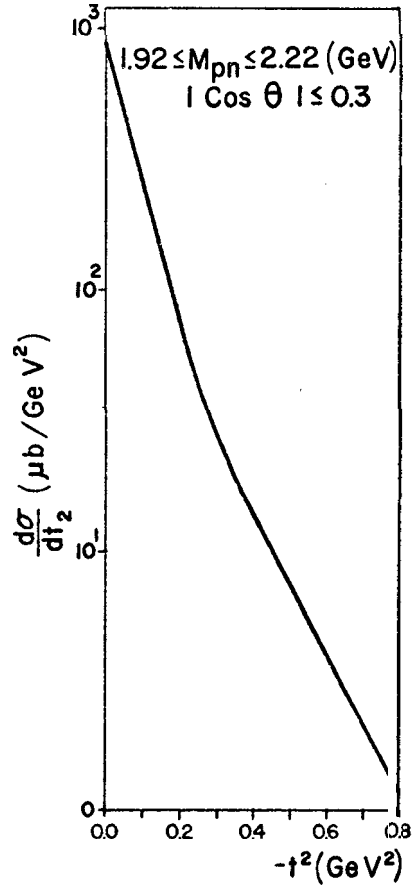


Fig.4 -  $d\sigma/dt_2$  distribution, integrated in  $\phi(0,2\pi)$ ,  $M_{pn}$  (1.92, 2.22 (GeV)) and  $|\cos \theta|$  (0,0.3).

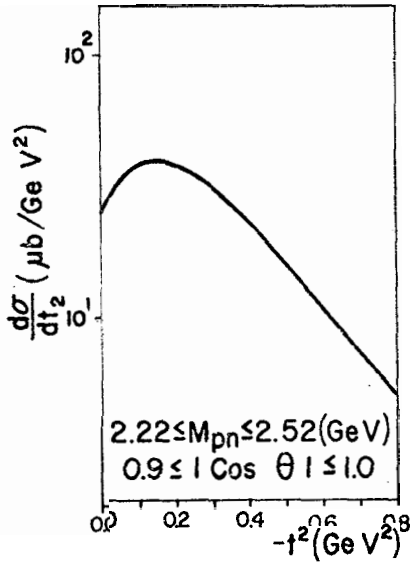


Fig.5 -  $d\sigma/dt_2$  distribution, integrated in  $\phi(0,2\pi)$ ,  $M_{pn}$  (2.22, 2.52 (GeV)) and  $|\cos\theta|(0.9,1.0)$ .

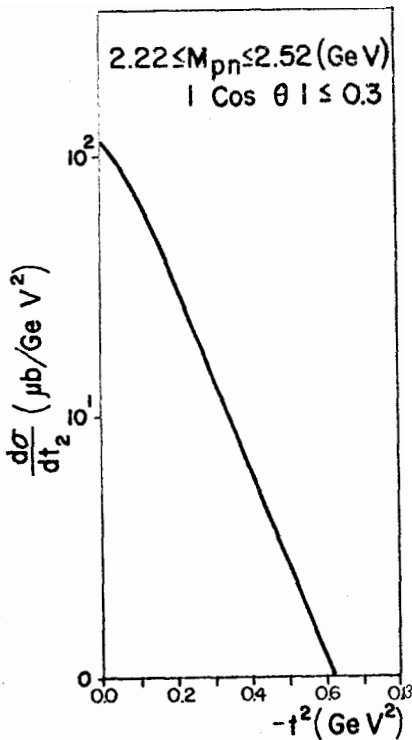


Fig.6 -  $d\sigma/dt_2$  distribution, integrated in  $\phi(0,2\pi)$ ,  $M_{pn}$  (2.22, 2.52 (GeV)) and  $|\cos\theta|(0,0.3)$ .

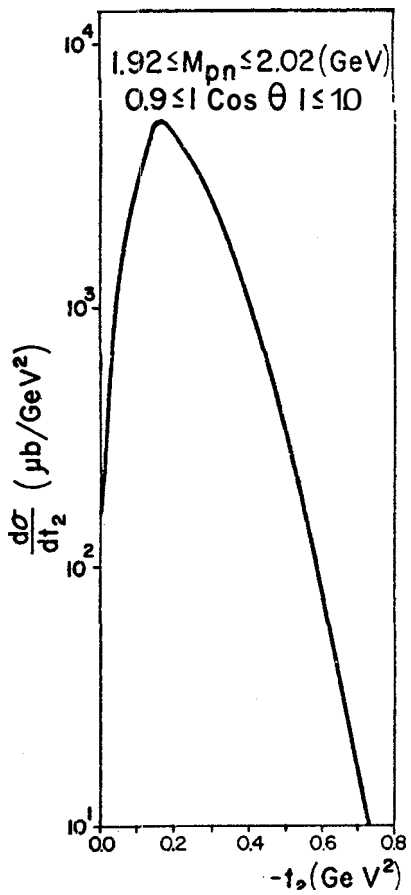


Fig.7 -  $d\sigma/dt_2$  distribution, integrated in  $\phi(0,2\pi)$ ,  $M_{pn}$  (1.92, 2.02 (GeV)) and  $|\cos\theta|$  (0.9,1.0).

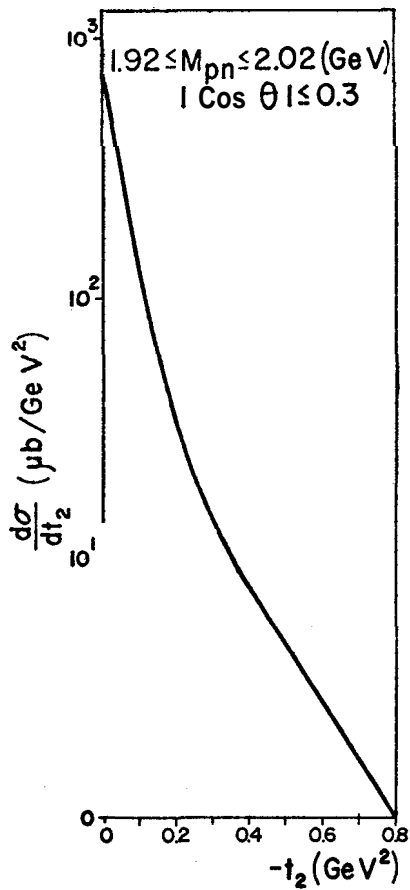


Fig.8 -  $d\sigma/dt_2$  distribution, integrated in  $\phi(0,2\pi)$ ,  $M_{pn}$  (1.92, 2.02 (GeV)) and  $|\cos\theta|$  (0,0.3).

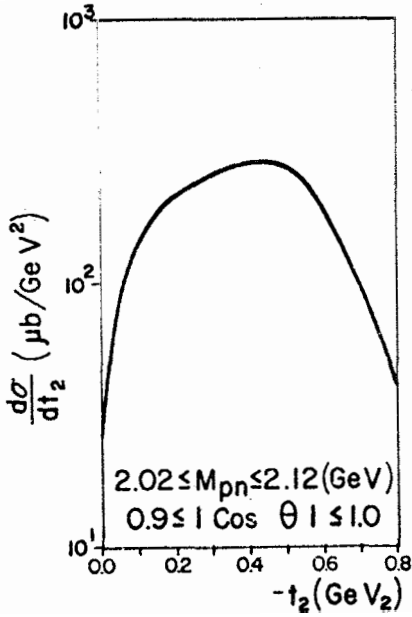


Fig.9 -  $d\sigma/dt_2$  distribution, integrated in  $\phi(0,2\pi)$ ,  $M_{pn}$  (2.02, 2.12 (GeV)) and  $|\cos \theta|$  (0.9, 1.0).

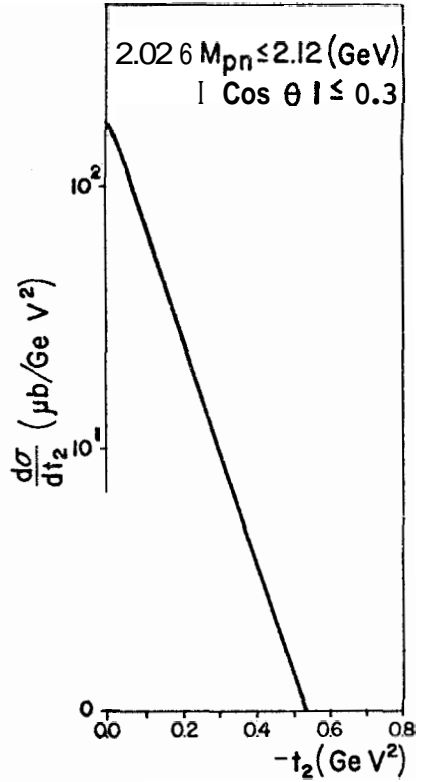


Fig.10 -  $d\sigma/dt_2$  distribution, integrated in  $\phi(0,2\pi)$ ,  $M_{pn}$  (2.02, 2.12 (GeV)) and  $\cos \theta|$  (0, 0.3).

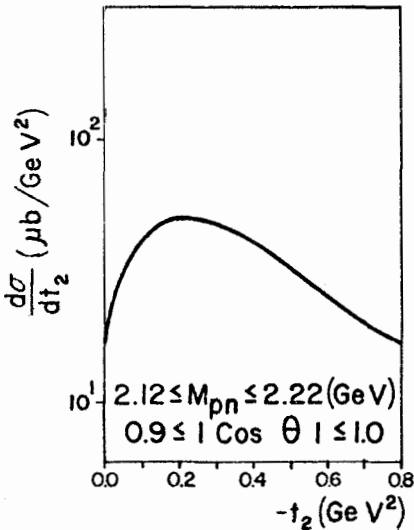


Fig.11 -  $d\sigma/dt_2$  distribution, integrated in  $\phi(0,2\pi)$ ,  $M_{pn}$  (2.12, 2.22 (GeV)) and  $|\cos \theta|$  (0.9, 1.0).

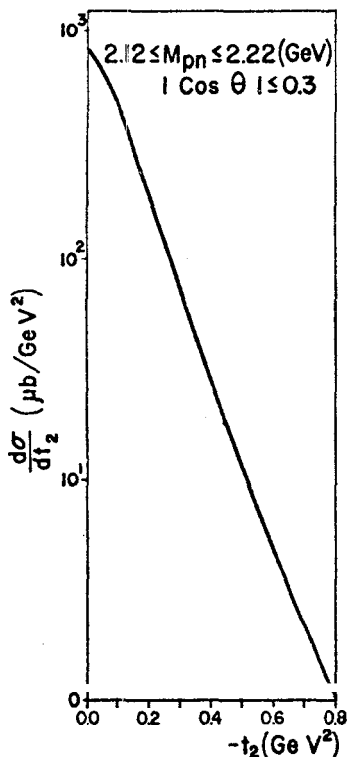


Fig.12 -  $d\sigma/dt_2$  distribution, integrated in  $\phi(0,2\pi)$ ,  $M_{pn}(2.12,2.22 \text{ GeV})$  and  $|\cos\theta|(0,0.3)$ .

This correlation is a consequence of destructive interferences among the three components of the model. A detailed discussion of these interferences effects is discussed elsewhere<sup>3b,4</sup>. The present results were calculated for 24 GeV protons in the laboratory system. This energy value is a typical one to assure the validity of the model. Notwithstanding, the amplitudes given here could be used to calculate the cross sections at other energies, in order to compare our results with experimental ones. We were unable to find experimental results to make this comparison.

The diffractive deuteron break up  $pd \rightarrow p(np)$  in the simplest example of light nuclei DDR. In the application of TDM to this reaction, the deuteron is treated as an elementary particle. If the predictions of the model presented here were confirmed, they would show the small contribution of the deuteron structure to the diffractive dissociation, as expected. This study could also be used to clarify some aspects concerning the applicability of nuclear democracy principle to the DDR.

The diffractive dissociation of deuteron is characterized by the kinematical region where it occurs, that is, high energy ( $s > 10 \text{ GeV}^2$ ), and small momentum transfer ( $-t, < 1 \text{ GeV}^2$ ). At this kinematical region the reaction is peripheral and the Regge phenomenology may be used. The small momentum transfer allows us to presume that the pomeron exchange dominates the process.

The diffractive cross section for deuteron break-up, obtained integrating the distribution of fig. 1 in the interval  $1.92 < M_{pn} < 2.52 \text{ GeV}$ , is  $\sigma_{\text{dif}} \approx 2.33 \text{ mb}$ .

An estimation of the non-diffractive cross section for this process, using a single scattering approximation and neglecting spin effects, gives  $\sigma_{\text{non-diff}} \approx 13 \text{ mb}$ .

Using a naive impulse approximation model without spin effects, with  $t_{pn}^{\text{elastic}}(t_2) = e^{-Bt_2}$ , to calculate the effective mass distribution due to the non diffractive contribution, we obtain a peak at the threshold. The height of this peak is about  $10 \text{ mb/GeV}$ , which may be compared with the  $39 \text{ mb/GeV}$  of the peak due to fig.1. The peak in  $d\sigma_{\text{non-dif}}/dM_{pn}$  behaves like  $(s_1 - m_d^2)^{-1}$ , similarly to that of  $d\sigma_{\text{dif}}/dM_{pn}$  near the threshold, but is broader, giving similar contribution to the integrated cross section. To observe the diffractive effects, use should be made of the difference in the shapes of the two peaks.

Finally we would like to stress that this is the first application of the TCDM to light nuclei diffractive dissociation, which enlarges the range of applicability of the model.

We would like to thank very much Profs. C. Alvear, J. Benuzzi, A. Santoro, M. Souza and S. Wulk for fruitful discussions and also thank Prof. J. Tiomno for a critical reading of the manuscript.



APPENDIX

This Appendix contains a summary of the kinematical variables and expressions useful to describe the deuteron diffractive break up.

The DDR  $a+b \rightarrow (1+2)+3$ , in general, and  $d+p \rightarrow (p+n)+p$  in particular, may be represented as in fig. (A1).

The TCDM which describes these reactions is represented by the diagrams of fig. (A2).

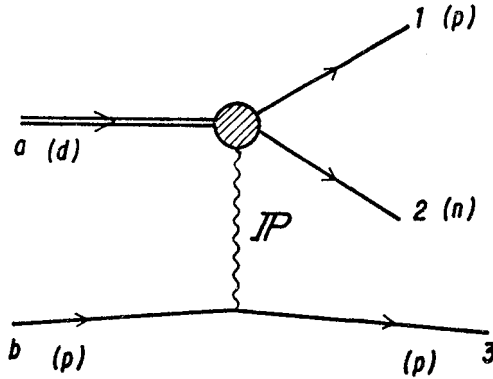


Fig.A1 -  $d+p \rightarrow p+n+p$  DDR, factorized by Pomeron exchange into the elastic vertex  $p \mathbb{P} p$  and the dissociation subreaction  $\mathbb{P} + d \rightarrow p + n$ .

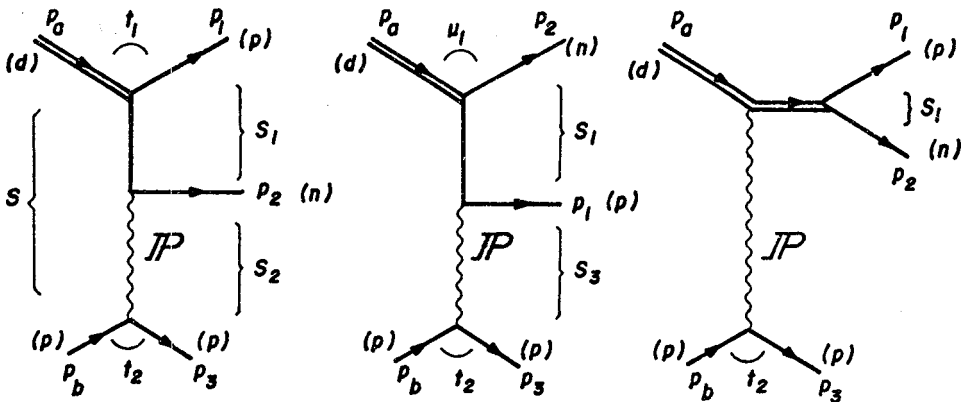


Fig.A2 - TCDM components which contribute to the DDR  $d+p \rightarrow p+n+p$ .

The fourmomenta corresponding to the external lines are  $p_i$  ( $i = a, b, 1, 2, 3$ ), and for the internal lines we define

$$q = p_a - p_1, \quad k = p_a - p_2 \quad \text{and} \quad p = p_1 + p_2 \quad (\text{A.1})$$

At the diffractive vertices the following fourmomenta are used

$$\begin{aligned} P &= (p_1 + k)/2, & Q &= (p_2 + q)/2 \\ K &= (p_a + p)/2 \quad \text{and} \quad R &= (p_b + p_3)/2 \end{aligned} \quad (\text{A.2})$$

Some invariants required to describe the TCM are

$$s = (p_a + p_b)^2, \quad s_1 = (p_1 + p_2)^2, \quad s_2 = (p_2 + p_3)^2$$

$$s_3 = (p_1 + p_3)^2, \quad t_1 = (p_a - p_1)^2, \quad u_1 = (p_a - p_2)^2$$

and

$$t_2 = (p_b - p_3)^2 \quad (\text{A.3})$$

The energies ( $E_i$ ) and the momenta  $|\vec{p}_i|$  ( $i = a, b, 1, 2, 3$ ) in the 12 system ( $\vec{p}_1 + \vec{p}_2 = 0$ ), as functions of the invariants are

$$E_a = (s_1 + m_a^2 - t_2)/2\sqrt{s_1}, \quad E_b = (s_1 - m_a^2 - m_3^2 + t_2)/2\sqrt{s_1}$$

$$E_1 = (s_1 + m_1^2 - m_2^2)/2\sqrt{s_1}, \quad E_2 = (s_1 + m_2^2 - m_1^2)/2\sqrt{s_1}$$

$$E_3 = (s - s_1 - m_3^2)/2\sqrt{s_1}, \quad |\vec{p}_a| = \lambda^{1/2}(s_1, m_a^2, t_2)/2\sqrt{s_1}$$

$$|\vec{p}_b| = \lambda^{1/2}(s_1, m_b^2, t_{a3})/2\sqrt{s_1}, \quad |\vec{p}_3| = \lambda^{1/2}(s_1, m_3^2, s)/2\sqrt{s_1}$$

and

$$|\vec{p}_1| = |\vec{p}_2| = \lambda^{1/2}(s_1, m_1^2, m_2^2)/2\sqrt{s_1} \quad (\text{A.4})$$

where

$$t_{a3} = s_1 - s - t_2 + m_a^2 + m_b^2 + m_3^2$$

and  $\lambda(x, y, z)$  is defined by

$$\lambda(x, y, z) = x^2 + y^2 + z^2 - 2(xy + xz + yz)$$

In the R12 system we define the Gottfried-Jackson system (GJS). The orientations of the axes are given by

$$\hat{z} = \vec{p}_a / |\vec{p}_a| \quad \text{and} \quad \hat{y} = (\vec{p}_3 \times \vec{p}_b) / |\vec{p}_3 \times \vec{p}_b| \quad (\text{A.5})$$

The angular coordinates of the momenta are

$$\vec{p}_1 = \vec{p}_1(\theta, \phi), \quad \vec{p}_b = \vec{p}_b(\chi, 0) \quad \text{and} \quad \vec{p}_3 = \vec{p}_3(\alpha, 0) \quad (\text{A.6})$$

The GJS is shown in figs. (A3).

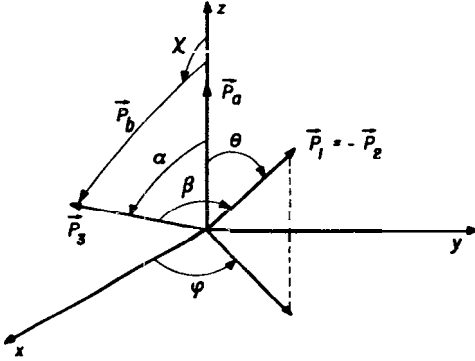


Fig.A3 - Angular coordinates of the momenta defined in the GJS.

High energy approximations are valid at the kinematical region characteristic of the DDR. They correspond to

$$s, s_2, s_3 \gg s_1, \quad |t_1|, |u_1|, |t_2|, \quad m_i^2 (i=a, b, 1, 2, 3) \quad (\text{A.7})$$

Within these approximations we have

$$2Q.R \approx s_2, \quad 2P.R \approx s_3 \quad \text{and} \quad 2K.R \approx s \quad (\text{A.8})$$

$$\cos \alpha \approx -(s_1 - m_a^2 + t_2) / \lambda^{1/2}(s_1, m_a^2, t_2) \quad \text{and}$$

$$\sin \alpha \approx 2\sqrt{s_1} \sqrt{-t_2} / \lambda^{1/2}(s_1, m_a^2, t_2) \quad (\text{A.9})$$

For a three particles final state reaction the cross-section is given by<sup>9</sup>

$$\sigma = C \int |A|^2 \frac{\lambda^{1/2}(s_1, m_1^2, m_2^2)}{s_1} ds_1 dt_2 d\cos \theta d\phi \quad (\text{A.10})$$

where

$$C = (2^{10} \pi^4 \lambda(s, m_a^2, m_b^2))^{-1}$$

## REFERENCES

1. G. Cohen-Tannoudji, A. Santoro and M. Souza, Nucl. Phys. **B125**, 445 (1977); G. Cohen-Tannoudji, D. Levy and M. Souza, Nucl. Phys. **B129**, 286 (1977).
2. G. Alberi and G. Goggi, Phys. Rep. **74**, 1 (1981).
3. a) A. Endler, M.A.R. Monteiro, A. Santoro and M. Souza, Z. fur Physik **C7**, 137 (1981); b) A.C. Antunes, A. Santoro and M. Souza, Rev. Bras. de Física **13**, 415 (1983) and ibid **13**, 601 (1983).
4. A.C. Antunes, A. Santoro and M. Souza, "Systematic of the slope-mass-correlations in diffractive dissociation reactions", in preparation.
5. G.F. Chew, *S-Matrix Theory of Strong Interactions*, (W.A. Benjamin Inc (N.Y.), 1961), and references therein; in B. de Witt and M. Jacob (eds.), *High energy physics*, Les Houches Lectures (Gordon and Breach, 1965).
6. M. Gourdin *et al.*, Nuovo Cim. **37**, 3240 (1965); G.W. Barry, Ann. of Phys. **73**, 482 (1972).
7. M.D. Scadron, Phys. Rev. **165**, 1640 (1968).
8. P.D.B. Collins, *An introduction to Regge Theory & High Energy Physics*, (Camb. Univ. Press. 1977).
9. E. Byckling and K. Kajantie, *Particle Kinematics*, (John Wiley, 1973).

## Resumo

A dissociação difrativa do deuteron é estudada no contexto do Modelo Deck a Três Componentes. Admite-se a aplicabilidade deste modelo à dissociação difrativa de núcleos leves. Observa-se a existência de uma correlação massa-inclinação-difrativa- $\cos\theta$ . Obtém-se as distribuições relevantes.